Discrete breathers in classical spin lattices

Y. Zolotaryuk and S. Flach

Max-Planck-Institut für Physik komplexer Systeme, Nöthnitzer Strasse 38, D-01187 Dresden, Germany

V. Fleurov

School of Physics and Astronomy, Raymond and Beverly Sackler Faculty of Exact Sciences, Tel-Aviv University, Tel-Aviv 69978, Israel

Discrete breathers (nonlinear localized modes) have been shown to exist in various nonlinear Hamiltonian lattice systems. In the present paper, we study the dynamics of classical spins interacting via the Heisenberg exchange on spatial d-dimensional lattices (with and without presence of single-ion anisotropy). We show that discrete breathers exist for the cases when the continuum theory does not allow for their presence (easy-axis ferromagnets with anisotropic exchange and easy-plane ferromagnets). We prove the existence of localized excitations, using the implicit function theorem, and obtain necessary conditions for this existence. The most interesting case is the easy-plane one, which yields excitations with locally tilted magnetization. There is no continuum analog for such a solution and there exists an energy threshold for it, which is estimated analytically. We support our analytical results with numerical high-precision computations, including also a stability analysis for the excitations.

I. INTRODUCTION

The phenomenon of dynamical localization has been a subject of intense theoretical research. It is well known that classical Hamiltonian lattices possess periodic-in-time and localized-in-space solutions called discrete breathers or intrinsic localized modes. A recent explosion of interest in discrete breathers has occurred due to the fact that they may exist in lattice models of interacting *identical* particles. Breathers in continuum models (for example, the well-known sine-Gordon equation) exist only due to high symmetry of the system, and therefore they are structurally unstable. Discrete breathers are generic solutions of nonlinear lattice equations. The existence of discrete breathers is based on the following fact. The band of small amplitude plane waves (BSAPW) above the classical ground state is bounded from above, and therefore it is possible that neither breather frequency nor any of its multiples will resonate with the BSAPW. So far, discrete breathers have been proven to be generic solutions in both Hamiltonian[1,2] and dissipative[3] systems. Several cases of experimental observation of discrete breathers have been reported [in Josephson junction arrays,[4] arrays of weakly coupled waveguides,[5] low-dimensional crystals,[6] and biological systems (myoglobin)[7]].

Due to spatial periodicity, the lattices of interacting spins are ideal systems to observe discrete breathers as well. Here, we will concentrate on large spins, which may be described classically. Nonlinear waves in magnetic systems have extensively been studied during the last three decades.[8,9] The results of these studies provide a lot of information about the properties of solitary waves (particularly, breathers) in magnets, since it is possible in many cases to obtain explicit solutions to them. However, neglecting discreteness effects may lead to loosing important features of nonlinear wave dynamics. For instance, since only high-symmetry continuous systems possess breather solutions, the area of potentially interesting models is artificially reduced. Another drawback of continuous systems is that the consideration of nontopological localized excitations is typically restricted to one-dimensional space.

In the last decade, a number of papers have appeared, where localized modes in magnets were treated as essentially discrete objects[10–12] (also, the attempt of experimental observation of discrete breathers in antiferromagnets has been made recently.[13]) However, no rigorous existence proofs have been given, and only the simplest cases (from the point of view of symmetries) have been considered. Preserving these symmetries, one can continue those solutions to the spatially continuous limit.

The aim of this work is to present breather excitations for spin lattices, for which the symmetries will not allow for a similar mode construction in spatially continuous cases. Also, we will not restrict the consideration to one-dimensional systems. Below, we present a rigorous existence proof for the discrete breathers in magnetic systems, using the anticontinuum limit. With the help of this proof and of the Newton iteration method, we show the existence of discrete breathers in ferromagnetic lattices with anisotropic exchange interaction. We also consider an easy-plane ferromagnet and find a new type of discrete breathers, with several spins precessing around the hard (single-ion anisotropy) axis, while all the others precess around an axis that lies in the easy plane. Note that only the simplest case of monochromatic-in-time breathers has been investigated in most of previous papers. This situation simplifies considerably the treatment of the system, and important families of solutions can be lost. Our studies do not depend in any way on the number of higher harmonics in the time evolution of a breather.

This paper is organized as follows. The next section presents the model Hamiltonian and the equations of motion. In Sec. III, we consider an easy-axis ferromagnet, discuss the

implementation of the anticontinuum limit, and give a rigorous proof for the existence of discrete breathers. In Sec. IV, we study an easy-plane ferromagnet. Section V presents the study of a two-dimensional lattice with easy-plane anisotropy. Discussions and conclusions are given in Sec. VI.

II. HAMILTONIAN AND EQUATIONS OF MOTION

We consider a lattice of classical spins described by the Hamiltonian with Heisenberg *XYZ* exchange interaction and single-ion anisotropy

$$H = -\frac{1}{2} \sum_{\mathbf{n} \neq \mathbf{n}'} \sum_{\alpha=(x,y,z)} J_\alpha^{\mathbf{nn}'} S_{\mathbf{n}}^\alpha S_{\mathbf{n}'}^\alpha - D \sum_{\mathbf{n}} S_{\mathbf{n}}^{z2}. \qquad (1)$$

Here $S_{\mathbf{n}}^x, S_{\mathbf{n}}^y, S_{\mathbf{n}}^z$ are the **n**th spin components (**n** labels lattice sites) that satisfy the normalization condition

$$S_{\mathbf{n}}^{x2} + S_{\mathbf{n}}^{y2} + S_{\mathbf{n}}^{z2} = S^2. \qquad (2)$$

For simplicity, the total spin magnitude can be normalized to unity: $S=1$. The constants $J_x, J_y, J_z > 0$ are the exchange integrals and D is the on-site anisotropy constant.

The equations of motion for the spin components in the one-dimensional spin chain with nearest-neighbor interactions are the well-known Landau-Lifshitz equations:

$$\dot{S}_n^x = \frac{1}{2}[J_y S_n^z(S_{n-1}^y + S_{n+1}^y) - J_z S_n^y(S_{n-1}^z + S_{n+1}^z)] - 2D S_n^y S_n^z,$$

$$\dot{S}_n^y = \frac{1}{2}[J_z S_n^x(S_{n-1}^z + S_{n+1}^z) - J_x S_n^z(S_{n-1}^x + S_{n+1}^x)] + 2D S_n^x S_n^z,$$

$$\dot{S}_n^z = \frac{1}{2}[J_x S_n^y(S_{n-1}^x + S_{n+1}^x) - J_y S_n^x(S_{n-1}^y + S_{n+1}^y)]. \qquad (3)$$

The generalization to higher lattice dimensions is straightforward.

III. EASY-AXIS FERROMAGNET

First, we consider spin lattices with the ground state that corresponds to all spins directed along a given axis (we assume this axis to be the Z axis). This can be achieved by introducing either a strong exchange anisotropy ($J_x, J_y \ll J_z$), or an on-site anisotropy term $D > 0$. Before we study the breather solutions of Eqs. (3), let us consider the dispersion laws for linear spin waves.

A. Dispersion laws

First, we consider the easiest case, the ferromagnetic chain without ion anisotropy ($D=0$), but with a strong exchange anisotropy: $0 \leq J_x, J_y \ll J_x$. In this case, the ground state is $S_n^z = \pm 1$, $S_n^x = S_n^y = 0$. Linearizing the equations of motion around one of these ground states, e.g., $S_n^x = \delta_x \sin(qn - \omega t)$, $S_n^y = \delta_y \cos(qn - \omega t)$, $S_n^z = \text{const} \approx 1$, we obtain

$$\omega_L^2(q) = (J_z - J_x \cos q)(J_z - J_y \cos q). \qquad (4)$$

This dispersion law is shown in Fig. 1, with the edges of the linear band $\omega_L(q)$ given by
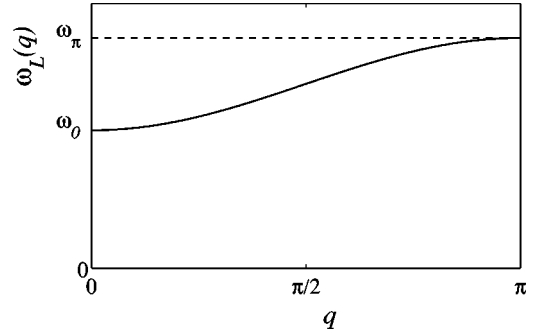

FIG. 1. Dispersion law for the ferromagnetic chain with strong exchange anisotropy.

$$\omega_0^2 = (J_z - J_x)(J_z - J_y), \quad \omega_\pi^2 = (J_x + J_z)(J_y + J_z). \qquad (5)$$

Let us explain how one can use the properties of the dispersion relations in order to formulate an outlook about the existence or nonexistence of breathers. It has been shown in Ref. 14 that the breather solutions of full nonlinear equations bifurcate from certain nonlinear plane-wave solutions. These specific plane-wave solutions are periodic in time and they are reduced to band edge plane waves (BEPW) in the limit of small amplitudes, linear waves with $\omega_L(q_{\text{BEPW}})$ being an extremum of $\omega_L(q)$. A necessary prerequisite for the existence of breathers is that the frequency of these BEPW's is split from the linear band $\omega_L(q)$ with an increasing amplitude or energy density of the wave.

Consider the excitation that corresponds to the wave number $q=0$. This is a spatially homogeneous excitation $S_n^\alpha = S^\alpha$ and the Landau-Lifshitz equations yield

$$\dot{S}^x = (J_y - J_z) S^y S^z,$$

$$\dot{S}^y = (J_z - J_x) S^x S^z,$$

$$\dot{S}^z = (J_x - J_y) S^x S^y. \qquad (6)$$

As can be seen from these equations, even for $J_x = J_y$ we have softening in the dispersion law at $q=0$. Then $\dot{S}^z = 0$, and for $S^x = A \cos \omega t$ (here A is the precession amplitude) the spin precession frequency given by

$$\omega^2 = (1 - A^2)(J_z - J_x)^2 < (J_z - J_x)^2 = \omega_0^2 \qquad (7)$$

appears to lie below the lower edge of the linear band, which suggests the occurrence of the discrete breathers in the band gap. Note that for the completely isotropic model $J_x = J_y = J_z \equiv J$, there is no gap and consequently no breather solutions are expected.

It is easy to check that a similar analysis of the upper band edge yields the lowering of the BEPW frequency with an increasing amplitude, i.e., the frequency is *attracted* by $\omega_L(q)$, instead of being repelled. Consequently, we do not expect breathers that could bifurcate from the upper band edge.

For $D \neq 0$, there are no qualitative changes. The ground state of the chain remains the same, whereas the gap in the dispersion law widens:

$$\omega_L^2(q) = (J_z - J_x \cos q)(J_z - J_y \cos q)$$
$$+ 4D\left(J_z - \frac{J_x + J_y}{2} \cos q\right) + 4D^2, \qquad (8)$$

with

$$\omega_0^2 = (J_z - J_x)(J_z - J_y) + 4D\left(J_z - \frac{J_x + J_y}{2}\right) + 4D^2,$$

$$\omega_\pi^2 = (J_x + J_z)(J_y + J_z) + 4D\left(J_x + \frac{J_x + J_y}{2}\right) + 4D^2. \qquad (9)$$

Note that the band gap exists even in the case of isotropic exchange (all J_α's are equal). Therefore, the easy axis anisotropy increases the changes of the breather existence.

B. Implementation of the anticontinuum limit

Now, following MacKay and Aubry,[15] we apply the approach based on the anticontinuum (AC) limit to our system. The main idea of the AC limit consists in decoupling the lattice sites and exciting only one or a small number of them, keeping all the other sites in the ground state. Then, upon switching on the interaction, the persistence of the localized solution is shown. As a prerequisite for the successful existence proof and continuation of the breather solution, the initial ''decoupled'' periodic orbit must be anharmonic[16] and the breather frequency and all its multiples should not resonate with the linear magnon band. In the case of strongly anisotropic exchange ($J_x, J_y \ll J_z$), the particular case of the AC limit means simply setting $J_x = J_y = 0$. In this case the Z component of each spin is conserved. The solution of Eqs. (3) reduces to the precession of decoupled spins around the Z axis with the frequencies that depend on the values of the Z components of nearest-neighbor spins (due to nonzero J_z):

$$S_n^x + iS_n^y = A_n e^{i(\omega_n t + \varphi_n)}, \quad \dot{S}_n^z = 0, \qquad (10)$$

where the precession frequency of the nth spin is given by

$$|\omega_n| = \frac{J_z}{2}(S_{n-1}^z + S_{n+1}^z) + 2DS_n^z, \quad A_n^2 = 1 - S_n^{z2}. \qquad (11)$$

Below, we consider the following three particular cases.

1. Single-ion anisotropy is absent ($D=0$)

The initial choice of one precessing spin and all the others being at rest, i.e.,

$$S_n^x = (\ldots, 1,1,1,S_0,1,1,1,\ldots) \qquad (12)$$

with $S_0 < 1$ cannot be used to generate breathers because the frequency of this solution $\omega = J_z$ resonates with the linear band [more precisely, with the lower edge of the linear band ω_0, see Eq. (5)]. Therefore it cannot be continued to the region of nonzero J_x and J_y. A way out is simply to excite three neighboring spins:

$$S_n^z = (\ldots, 1,1,1,S_1,S_0,S_1,1,1,1,\ldots). \qquad (13)$$

Here $0 < S_0 < S_1 < 1$ and, since the precession frequency of all the three central spins must be the same, we have $S_0 = 2S_1 - 1$. In this case, the precession frequency $\omega = J_z S_1$, allowing for the absence of resonances with the linear spectrum frequency $\omega_0 = J_z$, must satisfy the condition $k\omega \neq \omega_0$.

2. Single-ion anisotropy is present ($D>0$)

In this case, we may use the AC limit with the ansatz (12). The initial distribution of the Z-spin components are chosen as

$$S_n^z = (\ldots, 1,1,1,S_0,1,1,1,\ldots). \qquad (14)$$

Here one central spin precesses with the frequency $\omega = J_z + 2DS_0$, whereas all the other spins are supposed to be at rest. Small deviations from their equilibrium states yield the precession with the frequencies

$$\omega_1 = \omega_0 + \tfrac{1}{2}(S_0 - 1), \quad \omega_0 = J_z(1 + 2D), \qquad (15)$$

distributed along the lattice as follows:

$$\omega_n = (\ldots, \omega_0, \omega_0, \omega_1, \omega, \omega_1, \omega_0, \omega_0, \ldots). \qquad (16)$$

The discrete breathers can be continued from the AC limit if the following nonresonance conditions are satisfied:

$$k\omega \neq \omega_0, \quad k\omega \neq \omega_1, \quad k \in Z. \qquad (17)$$

Taking into account that $S_0 = (\omega - J_z)/2D$ and substituting it into the nonresonance condition $\omega \neq \omega_1$, we get

$$k\omega \neq \frac{J_z}{2} + 2D - \frac{J_z^2}{4D} + \frac{J_z}{4D}\omega$$

$$\equiv -4D\left(\frac{J_z}{4D} - 1\right)\left(\frac{J_z}{4D} + \frac{1}{2}\right) + \frac{J_z}{4D}\omega. \qquad (18)$$

Note that for $k=1$ the resonance will occur for any breather frequency if $J_z = 4D$. For this set of parameters, the breather continuation from the AC limit is not possible for any frequency. For this particular case, we try another ansatz, namely, the even-parity pattern:

$$S_n^z = (\ldots, 1,1,1,S_0,S_0,1,1,1,\ldots),$$

$$\omega_n = (\ldots, \omega_0, \omega_0, \omega_1, \omega, \omega, \omega_1, \omega_0, \omega_0, \ldots) \qquad (19)$$

with ω_0 and ω_1 being the same as in Eq. (15), and

$$\omega = \frac{J_z}{2}(1 + S_0) + 2DS_0. \qquad (20)$$

Then, using the nonresonance condition (17), which is valid for this ansatz as well, we obtain

$$k\omega \neq \omega_1 = \frac{(J_z + 4D)^2 - J_z^2}{2(J_z + 4D)} + \frac{J_z}{J_z + 4D}\omega. \qquad (21)$$

It follows from this expression that the even-parity AC limit allows for continuation of the breather solution for all values of J_z and D.

3. Isotropic exchange ($J_x = J_y = J_z \equiv J$)

Here the ansatz (12) can be used and the frequencies in the AC limit will be distributed as $\omega_n = 2DS_n^z$. The eigenfrequencies of the nonexcited spins do not depend on the values of the adjacent spins and equal ω_0. Thus, the only nonresonance condition to be fulfilled is $k\omega \neq \omega_0$.

C. Existence proof for magnetic breathers

Here we present the rigorous proof of the existence of the discrete breathers in the particular case of strongly anisotropic exchange and $D > 0$.

Theorem 1. *If a periodic orbit of the Hamiltonian* (1) *with a frequency* ω *is nonresonant* [$k\omega \neq \omega_{0,1}$, $k \in Z$ *and* $\omega_L(q)$] *and anharmonic,*[16] *then the periodic orbit of the equations of motion* (3) *at* $\alpha \equiv \{J_x, J_y\} = 0$ *given by the spin-precession distribution* (13) *has a locally unique continuation as a periodic orbit of the equations* (3) *with the same period* $T = 2\pi/\omega$ *for a sufficiently small* α.

Proof: Let SL_T be the space of bounded infinite sequences $z \equiv \{z_n\}_{n \in Z}$ of triplets $z_n = (S_n^x, S_n^y, S_n^z)$ of continuously differentiable functions of a period $T = 2\pi/\omega$ with the symmetry properties:

$$S_n^x(t) = S_n^x(-t), \quad S_n^y(t) = -S_n^y(-t), \quad S_n^z = S_n^z(-t). \tag{22}$$

Then, the size of oscillations on the nth site will be measured by the following norm:

$$|z_n| = \sup\{|S_n^x(t)|, |S_n^y(t)|, |\dot{S}_n^x(t)|, |\dot{S}_n^y(t)|; t \in R\}. \tag{23}$$

Next, the size of $z \in SL_T$ is given by

$$|z| = \sup\{|z_n|; n \in Z\} \tag{24}$$

and therefore SL_T is a Banach space.

Consider now another Banach space SM_T of bounded infinite sequences $w \equiv \{w_n\}_{n \in Z}$ of triplets $w_n = (M_n^x, M_n^y, M_n^z)$ of continuous functions of a period T with the symmetry properties:

$$M_n^x(t) = -M_n^x(-t), \quad M_n^y(t) = M_n^y(-t), \quad M_n^z = -M_n^z(-t), \tag{25}$$

and the norms:

$$|w_n| = \sup\{|M_n^x(t)|, |M_n^y(t)|, |M_n^z(t) - 1|; t \in R\},$$

$$|\omega| = \sup\{|w_n|; n \in Z\}. \tag{26}$$

Define the mapping F: $SL_T \to SM_T$ defined by

$$F(z, \alpha) = w$$

with

$$\alpha = \{J_x, J_y\}, \quad z = \{S_n^x, S_n^y, S_n^z\}_{n \in Z}, \quad w = \{M_n^x, M_n^y, M_n^z\}_{n \in Z},$$

where

$$M_n^x = \tfrac{1}{2}[J_y S_n^z(S_{n-1}^y + S_{n+1}^y) - J_z S_n^y(S_{n-1}^z + S_{n+1}^z)]$$
$$- 2DS_n^y S_n^x - \dot{S}_n^x,$$

$$M_n^y = \tfrac{1}{2}[J_z S_n^x(S_{n-1}^z + S_{n+1}^z) - J_x S_n^z(S_{n-1}^x + S_{n+1}^x)]$$
$$+ 2DS_n^x S_n^x - \dot{S}_n^y,$$

$$M_n^z = \tfrac{1}{2}[J_x S_n^y(S_{n-1}^x + S_{n+1}^x) - J_y S_n^x(S_{n-1}^y + S_{n+1}^y)] - \dot{S}_n^z. \tag{27}$$

The symmetric solutions of the equations of motion (3) are in one-to-one correspondence with zeros of F, i.e., $F(z, \alpha) = 0$, especially in the case when $\alpha = 0$. Using the implicit function theorem, we prove this solution to have a locally unique continuation $z(\alpha)$ for sufficiently small α, such that $F[z(\alpha), \alpha] = 0$ provided $F \in C^1$ and its derivative with respect to z, $\mathcal{D}$, is invertible at $\alpha = 0$.

To show the invertibility of $\mathcal{D}F$, we linearize the map around the periodic orbit at $\alpha = 0$, so that

$$\delta \mathbf{M} = \mathcal{D}F \, \delta \mathbf{S}, \tag{28}$$

and show that it is invertible simultaneously in the following three parts of the lattice: the central site $n = 0$, its adjacent sites $n = \pm 1$, and the remainder of the lattice. The invertibility of $\mathcal{D}F$ is equivalent to the invertibility of the corresponding matrix in Eq. (28).

(i) For $n \neq 0, \pm 1$ we have

$$\delta M_n^x = -\delta S_n^y \omega_0 - \delta \dot{S}_n^x,$$

$$\delta M_n^y = \delta S_n^x \omega_0 - \delta \dot{S}_n^y, \tag{29}$$

$$\delta M_n^z = -\delta \dot{S}_n^x.$$

Since the functions δM_n^α and δS_n^α are periodic in time, one can expand them into Fourier series

$$\delta \cdots = \sum_{k=-\infty}^{+\infty} \delta \cdots (k) e^{ik\omega t}. \tag{30}$$

The time-symmetry requirements (22) ensure $\delta \cdots (k \geq 0)$ to be either purely real or imaginary, so that

$$\delta M_n^x(-k) = \delta M_n^x(k), \quad \delta M_n^y(-k) = \delta M_n^y(k),$$

$$\delta M_n^z(-k) = -\delta M_n^z(k),$$

$$\delta S_n^x(-k) = \delta S_n^x(k), \quad \delta S_n^y(-k) = -\delta S_n^y(k),$$

$$\delta S_n^z(-k) = \delta S_n^z(k). \tag{31}$$

Particularly, $\delta M_n^x(0) = \delta M_n^z(0) = \delta S_n^y(0) = 0$. As a result, for $k \geq 0$ we obtain

$$\delta M_n^x(k) = -\omega_0 \delta S_n^y(k) - ik\omega \delta S_n^x(k),$$

$$\delta M_n^y(k) = \omega_0 \delta S_n^x(k) - ik\omega \delta S_n^y(k),$$

$$\delta M_n^z(k) = -ik\omega \delta S_n^z(k). \quad (32)$$

These equations appear to be decoupled with respect to k and they can be inverted in $k^2\omega^2 \neq \omega_0^2$. The third equation can be inverted for $k \neq 0$ if $\omega \neq 0$. For $k = 0$ the inversion is impossible, but this degeneracy can be lifted by imposing the normalization condition (2). In fact, the third equation can be dropped because S_n^z is defined by S_n^x and S_n^y with accuracy up to a sign. All that we have to check is the inequality $S_n^{x^2} + S_n^{y^2} - 1 \leq 0$.

(ii) For $n = \pm 1$ we act similarly to the previous case:

$$\delta M_1^x = -\delta S_1^y \omega_1 - \delta \dot{S}_1^x,$$

$$\delta M_1^y = \delta S_1^x \omega_1 - \delta \dot{S}_1^y,$$

$$\delta M_1^z = -\delta \dot{S}_1^x. \quad (33)$$

The similar condition for invertibility can be found: $k^2\omega^2 \neq \omega_1^2$.

(iii) Case $n = 0$. Using the canonical coordinate y and momentum p given by

$$S_0^x = \sqrt{1-y^2}\cos p, \quad S_0^y = \sqrt{1-y^2}\sin p, \quad S_0^z = y, \quad (34)$$

one obtains the following Hamilton equations:

$$\dot{y} = \frac{\partial H}{\partial p}, \quad \dot{p} = -\frac{\partial H}{\partial y}. \quad (35)$$

Next, we define the pair (u,v), instead of the set (M_0^x, M_0^y, M_0^z), with

$$u = \frac{\partial H}{\partial p} - \dot{y}, \quad v = -\dot{p} - \frac{\partial H}{\partial y}. \quad (36)$$

The new function $y(t)$ satisfies the following symmetries:

$$y(t) = y(-t), \quad p = \omega t + h(t), \quad h(t) = -h(-t),$$

$$y(t+T) = y(t), \quad h(t) = h(t+T). \quad (37)$$

Here $h(t)$ is a periodic function in time. Keeping in mind that S_{-1}^z and S_1^z are fixed by variations of $S_{\pm 1}^{x,y}$, we obtain

$$\delta u = 2D\,\delta y - \delta \dot{p} = 2D\,\delta y - \delta \dot{h},$$

$$\delta v = -\delta \dot{y}. \quad (38)$$

After considering the corresponding Fourier series with respect to time, we find the following inversion conditions: $\omega \neq 0$ for $k \neq 0$ and $D \neq 0$ for $k = 0$.

Once the invertibility is shown, by the implicit function theorem, the initial solution $z(0)$ has a locally unique continuation $z(\alpha)$ in SL_T, and thus the theorem has been proved.

This result can easily be extended to lattices in higher dimensions, antiferromagnets, and systems with larger interaction radius.

D. Method of computation of discrete breathers and linear stability analysis

For numerical simulations it is convenient to use stereographic coordinates. The new coordinates incorporate the normalization condition and reduce the problem with three unknown real functions per site to the problem with one unknown complex function per site:

$$\xi_n = \frac{S_n^x + iS_n^y}{1 + S_n^z}. \quad (39)$$

The inverse transform is given by

$$S_n^x = \frac{\xi_n + \xi_n^*}{1 + |\xi_n|^2}, \quad S_n^y = \frac{1}{i}\frac{\xi_n - \xi_n^*}{1 + |\xi_n|^2}, \quad S_n^z = \frac{1 - |\xi_n|^2}{1 + |\xi_n|^2}. \quad (40)$$

In these new coordinates the Landau-Lifshitz equations take the form

$$\dot{\xi}_n = \frac{1}{4i}\left[(J_x + J_y)\left(\frac{\xi_{n-1} - \xi_n^2 \xi_{n-1}^*}{1 + |\xi_{n-1}|^2} + \frac{\xi_{n+1} - \xi_n^2 \xi_{n+1}^*}{1 + |\xi_{n+1}|^2} \right) \right.$$
$$+ (J_x - J_y)\left(\frac{\xi_{n-1}^* - \xi_n^2 \xi_{n-1}}{1 + |\xi_{n-1}|^2} + \frac{\xi_{n+1}^* - \xi_n^2 \xi_{n+1}}{1 + |\xi_{n+1}|^2} \right)$$
$$\left. - 2J_z\xi_n\left(\frac{1 - |\xi_{n-1}|^2}{1 + |\xi_{n-1}|^2} + \frac{1 - |\xi_{n+1}|^2}{1 + |\xi_{n+1}|^2} \right) - 8D\xi_n\frac{1 - |\xi_n|^2}{1 + |\xi_n|^2} \right]. \quad (41)$$

The computation of the discrete breathers is done, using the Newton map.[1]

The linear stability analysis of the discrete breathers is performed by linearizing Eqs. (41): $\xi_n(t) = \xi_n^{(0)}(t) + \epsilon_n(t)$ around the breather periodic orbit, and solving afterwards the eigenvalue problem

$$\begin{pmatrix} \operatorname{Re}\epsilon_n(T) \\ \operatorname{Im}\epsilon_n(T) \end{pmatrix} = \hat{\mathcal{M}}\begin{pmatrix} \operatorname{Re}\epsilon_n(0) \\ \operatorname{Im}\epsilon_n(0) \end{pmatrix}. \quad (42)$$

If the eigenvalues Λ of the Floquet matrix $\hat{\mathcal{M}}$ are found to be located on the unit circle of the complex plane, then according to the Floquet theorem, the periodic orbit is stable, otherwise it is unstable.

E. Breather solutions in an easy-axis ferromagnet

Breathers in magnetic lattices with an easy-axis anisotropy can be viewed as localized spin excitations with the spins precessing around one of the ground states of the system (which was chosen in Sec. III to be $S^z = 1$), so that the effective radius of this precession decreases to zero as $n \rightarrow \pm\infty$. The case of an isotropic exchange in XY ($J_x = J_y$) is the simplest one because the S^z component is conserved in the solution, and therefore the separation of the time and the space variables
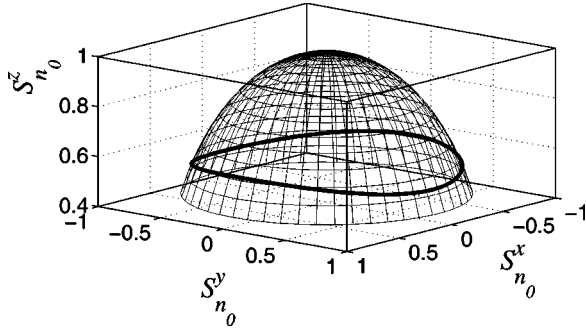
FIG. 2. Dynamics of the central spin with site number $n_0 = 11$ in the chain of $N = 21$ spins with $J_x = 0.1$, $J_y = 0.23$, $J_z = 1$, and $D = 0$.

$$S_n^+ = S_n^x + i S_n^y = A_n e^{i \omega t} \tag{43}$$

is possible in the Landau-Lifshitz equation [this can easily be seen also from Eq. (41)]. The precession amplitudes A_n do not depend on time and the Landau-Lifshitz equations (3) are reduced to a set of algebraic equations that can be solved by a simple iteration procedure. This is true both in the case of strong exchange anisotropy $J_x = J_y \ll J_z$ and also when the exchange is isotropic and the on-site anisotropy $D > 0$ is present.

The breather existence in the $J_{x,y}$-D plane is governed by the nonresonance conditions given in Sec. III B for the single harmonic $k = 1$. With the growth of $J_{x,y}$, the breather frequency may hit the linear spectrum that marks the boundary of the breather existence on this plane. The nature of the other nonresonance condition (18) is different, e.g., we cannot continue the breather solution for small $J_{x,y}$ when $J_z = 4D$, however, the breathers exist for larger values of $J_{x,y}$. Note that in the case of $J_x = J_y$, the discrete breathers have a continuum equivalent that is the breather solution of the integrable nonlinear Schrödinger equation. The reason is that the XY exchange symmetry allows one to find solutions that are monochromatic in time [see Eq. (43)]. As long as the linear band provides a gap and the nonlinearity allows for pushing the breather frequency into the gap, localized excitations may be found regardless of the degree of discreteness of the system, which can be characterized by the ratio of the gap to the bandwidth of the spin wave spectrum.

Now we consider a rhombic chain with $J_x \neq J_y < J_z$. Breaking isotropy in the XY plane implies that S^z is not conserved in the solution anymore, and according to the Landau-Lifshitz equations, it is impossible to represent the breather solution in the form (43). This implies that the breathers will have an infinite number of harmonics in time, and consequently the spin dynamics is more complicated. Each spin now draws an ''elliptic'' trajectory on the unit sphere, elongated toward the larger component of J_x or J_y. Figure 2 shows the dynamics of the central spin $n_0 = 11$ of the breather in the chain consisting of $N = 21$ spins. The breather profile at some instant of time is shown in Fig. 3.

Due to the broken symmetry in the XY plane, we are not able to find the breathers in the corresponding continuum problem. The reason simply is that the linear band of continuum equations may still have a gap, but will be un-
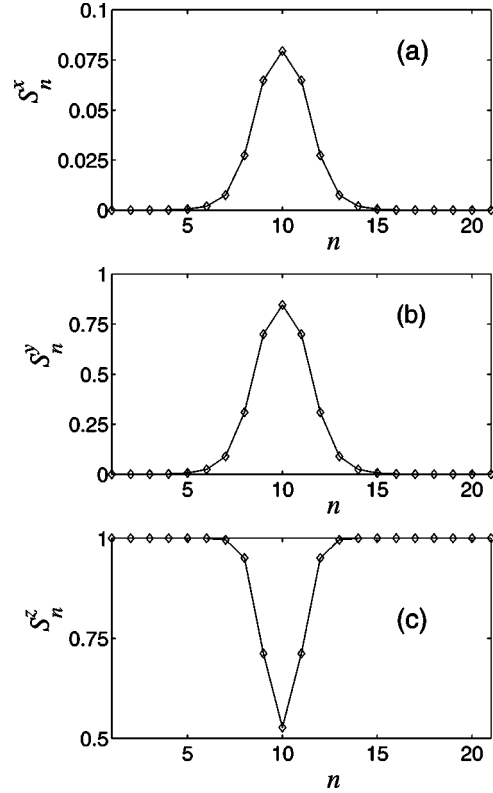

FIG. 3. Discrete breather profile at a fixed instant of time for the parameters described in Fig. 2.

bounded from above. Consequently, there will be unavoidable resonances of higher harmonics of the breather with the linear band, causing in general nonexistence of the breather solution itself. Here we have a nontrivial case, where the discreteness of the lattice provides the necessary support for the breather existence, which is missing in the continuum case. The computation of the breather periodic orbits in this case cannot be reduced to solving a system of algebraic equations and we have to work in the full phase space, using, e.g., a generalized Newton map.[1]

Let us briefly discuss now the stability of the obtained breather solutions. The previous stability studies[17] have shown that the stability depends on the breather parity (i.e., its spatial symmetry). The Floquet analysis of the eigenvalues of the stability matrix for our solutions confirms these findings. We obtain that the site-centered breathers (continued from the one-site breather) are stable in the limit of small exchange [see Fig. 4(a)], whereas the bond-centered breathers [continued from the two-site breathers, see the ansatz (19] are unstable arbitrarily close the AC limit, with the unstable eigenvalue being located on the positive half or the real axis outside the unit circle [see Fig. 4(b)].

IV. EASY-PLANE FERROMAGNET

In the case of an easy-plane anisotropy, we choose $D < 0$ and $J_x = J_y = J_z \equiv J$. Without loss of generality, the ground state of the system can be assumed to be
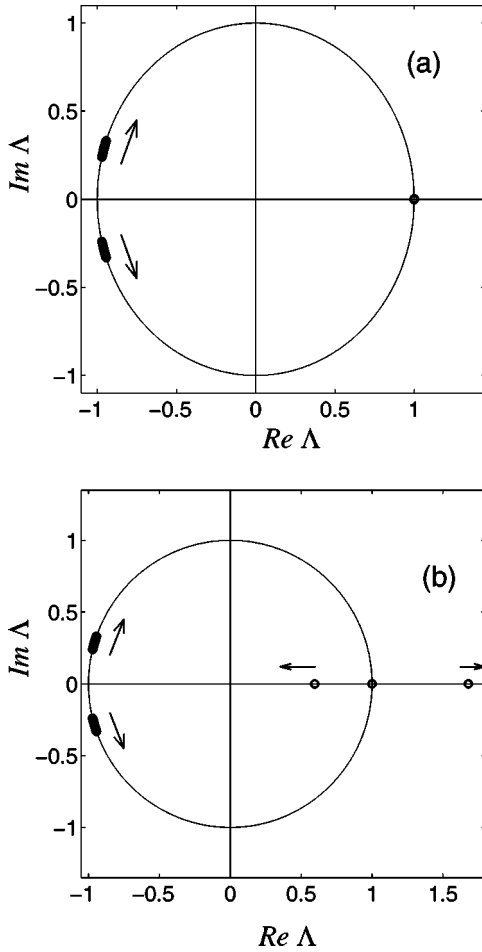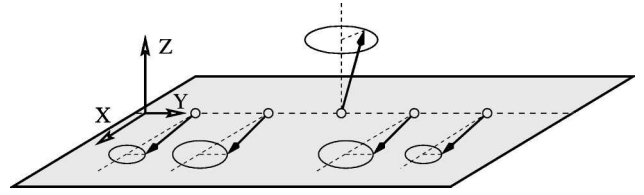
FIG. 5. Schematic representation of the discrete breather with one ''out-of-plane'' spin in easy-plane ferromagnet.

If the nonresonance condition $\omega \neq \omega_\pi = 0$ is satisfied, the breather solution can be continued.

In the continuum limit, breathers are not known to exist in ferromagnets with easy plane anisotropy.[18,19] The reason is again that the corresponding linear band is gapless and unbounded, so that it covers the whole real axis. Correspondingly, there is no place for the frequency of a localized excitation on the real axis that does not resonate with the linear band. An essentially discrete model[11] has been studied only in the case of a strong magnetic field directed along the hard axis. In this case, the hard axis effectively becomes an easy axis and, as a result, the spins precess around the Z axis with a constant S^z component. Here the separation of the variables (43) is possible that simplifies the treatment of the system.

B. Breather solutions of the easy-plane ferromagnet

As stated above, we do not apply an external magnetic field, and therefore we do not change the ground state. As in the previous case of easy-axis, we compute the breather periodic orbits from the AC limit, using a generalized Newton method. As a result, we obtain the solutions for one or two parallelly precessing ''out-of-plane'' spins shown in Figs. 5 and 6, respectively.

For nonzero J, initially nonexcited spins start to precess with small amplitudes around the X axis, while the plane of precession of the out-of-plane spin is no longer parallel to the easy plane, being slightly tilted. The breathers with more than two precessing spins can also be created.

Depending on its frequency, the breather width changes. When the frequency approaches the upper edge of the linear band, the breather becomes more delocalized. However, this does not qualitatively influence its core structure, i.e., the effective precessing axis of the central spin is not continuously tilted toward the X-axis upon lowering the breather frequency down the linear band edge. The central spin dynamics can be viewed as a periodic (closed orbit of a point confined to the unit sphere. Let the XY plane be the equato-

FIG. 4. Eigenvalues $\{\Lambda\}$ of the Floquet matrix for (a) site-centered breather and (b) bond-centered breather in the easy-axis chain of $N = 32$ spins with $D = 1$, $J = 0.01$, and $\omega = 1.3$. Arrows show direction of motion of eigenvalues when J increases.

$$S_n^x = 1, \quad S_n^y = S_n^z = 0. \tag{44}$$

Note that the ground state is degenerate, so that the spins can be oriented arbitrarily in the XY plane, but they must stay parallelly to each other.

A. Linear dispersion law and the anticontinuum limit

Linearizing the equations of motion in the vicinity of the ground state (44), we obtain the following dispersion law:

$$\omega^2(q) = J^2(1 - \cos q)^2 + 2J|D|(1 - \cos q). \tag{45}$$

This is an ''acoustic''-type dispersion law with

$$\omega_0^2 = \omega^2(0) = 0, \quad \omega_\pi^2 = \omega^2(\pi) = 4J(J + |D|), \tag{46}$$

and therefore the breather frequencies in this case should lie above the linear band.

The implementation of the AC limit can be achieved by setting $J = 0$ and exciting one or several spins, so that they should start to precess around the hard axis with the frequency $\omega = 2|D|S_0$, where S_0 is the z projection of the spin.
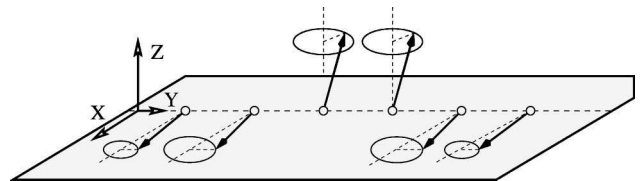

FIG. 6. Schematic representation of the discrete breather with two parallel out-of-plane spins in easy-plane ferromagnet.
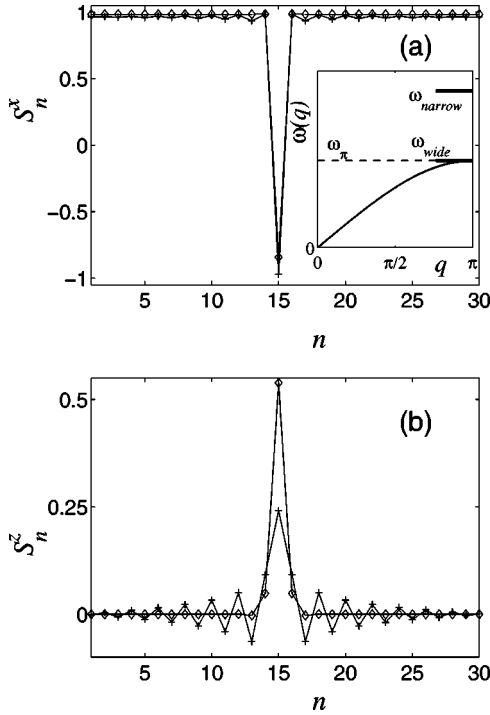
FIG. 7. Discrete breather profile $J=0.1$, $D=-1$, ω_{narrow} $=1.1967$ (diamonds), and $\omega_{\text{wide}}=0.6649$ (crosses). Inset shows the linear dispersion law and the location of breather frequencies.

rial one. Then for large breather frequencies, the point performs small circles around the north (or south) pole. Lowering the breather frequency does not change the fact that the loop still encircles the Z axis. Thus, the breather solution cannot be deformed into a slightly perturbed and weakly localized BEPW. This makes clear that the easy-plane ferromagnet lattice supports the breather solutions with a local magnetization tilt that have no analog in the continuum theory. The situation is illustrated by Fig. 7, where the profiles of two breathers are represented: one corresponds to the frequency $\omega_{\text{wide}}=0.6649$, which is very close to the upper edge of the linear band with $\omega_\pi=0.6633$, and the other one has the frequency $\omega_{\text{narrow}}=1.1967$, which is far above the linear band (see the insert in Fig. 7).

The first solution is more delocalized, which can be seen in Fig. 7. However, the central spin still precesses in a way similar to the ''narrow'' breather, i.e., it encircles the north pole on some lower latitude as compared to the narrow breather (see Fig. 8, where the two curves on the unit sphere correspond to the two breather-periodic orbits discussed above).

Hence, even when very close to the linear band, our breather solutions have the structure that has no analog in the continuum case. Moreover, we have investigated the dependence of the breather energy on the breather frequency (see Fig. 9). We observe that there exists an energy threshold, since the breather energy attains a nonzero minimum, when its frequency is still not equal to the edge of the linear-spin-wave spectrum. Note that for lattices of interacting scalar degrees of freedom, the discrete breathers have typically zero lower-energy bounds in spatial dimension $d=1$ and become
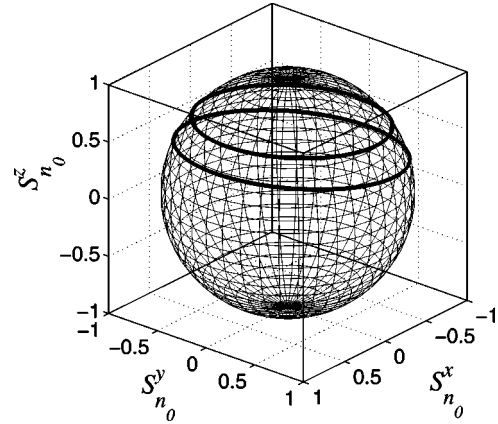

FIG. 8. Dynamics of the central spin with site number $n_0=15$ in the chain described in Fig. 7.

nonzero only for $d=2,3$.[20] The reason for the appearance of a nonzero lower bound in the present case is due to the already mentioned fact that the breather of the easy-plane ferromagnet system is not deformed into a perturbed-band-edge magnon wave. Instead, the central spin (s) is precessing around the Z axis. This topological difference is the reason for the appearance of nonzero lower energy bounds. Such energy thresholds may be very important as they show up in contributions to thermodynamic quantities that depend exponentially on temperature. To eliminate possible size effects, we repeated the calculations demonstrated in Fig. 9 for a chain with $N=50$ spins. The difference between the curves was negligibly small.

Energy thresholds can be estimated analytically in the limit of small exchange J. Ignoring the displacements of all in-plane spins, we obtain the threshold energy for the breather with M out-of-plane precessing spins, normalized to the ground state with

$$E(\omega) \approx 2M|D|S_0^{z\,2}, \tag{47}$$

where $S_0^z=\omega/2|D|$ is the Z component of the precessing spin in the AC limit [see Eq. (3)]. The factor 2 comes from the fact that we should take into account the contribution of the breather tails.
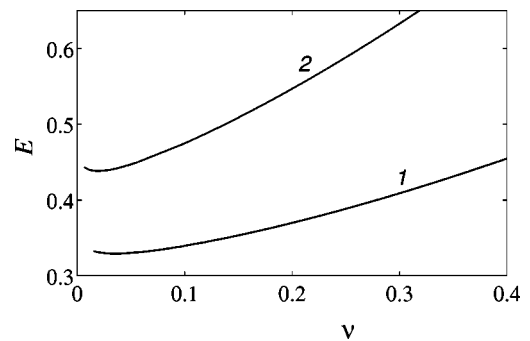

FIG. 9. Normalized energy $E=H+JN/2$ as a function of the detuning frequency $\nu=\omega-\omega_\pi$ for a discrete breather with one out-of-plane spin (curve 1) and with two out-of-plane spins (curve 2) for $J=0.1$. The size of the system is $N=30$ spins.

Equation (47) can be obtained, using the following arguments. For large values of ν in Fig. 9, the main contribution to the breather energy comes from the M out-of-plane precessing spins because the tail amplitudes of the breather are small (see, for example, Fig. 7). For $\nu \to 0$, the energy contribution from the tails is actually diverging. Thus, the height of the minima of the curves in Fig. 9 can be estimated as two times the contribution coming from the central spins. The substitution into the above formula for the band edge frequency ω_π yields $E = E(\omega_\pi) \approx 2MJ + O(J^2)$. For the case considered in Fig. 7, for $M = 1$ (one precessing spin) the analytic result yields $E \approx 0.2$, while the numerics give the value 0.33. In the case of two precessing spins ($M = 2$), the numerical result yields $E \approx 0.44$, whereas the analytical estimate predicts the value 0.4.

Increase of the frequency leads to decrease of the precession radius of the central spin. In the AC limit, the upper bound for the breather frequency is determined by $\omega = 2D$ that corresponds to the central (precessing) spin being parallel to the Z axis. This bound continues to exist when the exchange is switched on. After reaching this frequency threshold, the breather becomes a stationary (time-independent) solution. The existence of such a solution has been verified numerically by solving the time-independent Landau-Lifshitz equations.

C. Stability of breather solutions and their asymptotic properties

We have investigated the stability of our solutions with the help of the Floquet analysis (for details, see Sec. III D), using direct Runge-Kutta simulations. For small J, the breathers with one precessing spin appear to be unstable (see Fig. 5), whereas the configuration that corresponds to two parallel precessing spins (see Fig. 6) is stable. Note that similar results have been obtained for the FPU-type lattices.[21]

Stability tests also included the following numerical experiment. The periodic breather orbit $\{S_n^x(t)^{(0)}, S_n^y(t)^{(0)}, S_n^z(t)^{(0)}\}$ is perturbed by deviating one of the central spins $S_n^z(0)^{(0)} - S_n^z(0)^{(0)} + \varepsilon$ and simulating the equations of motion (3). The error function

$$\Delta(t) = \min_{\tau \in [0,T]} \left(\sum_{n=1}^{N} \sum_{\alpha = (x,y,z)} [S_n^\alpha(t) - S_n^{\alpha(0)}(\tau)]^2 \right)^{1/2} \tag{48}$$

was calculated on each breather oscillation period T. In Fig. 10, such a function (with $\varepsilon = -0.0025$, in a chain consisting of $N = 1000$ spins with periodic boundary conditions) is shown for the breather solution with two in-phase precessing spins (see Fig. 6).

The error function is bounded during significant time period (more than 10 000 breather oscillation periods) and the breather structure remains preserved. The similar numerical experiments have been performed for other types of breathers. They yield similar results. This demonstrates the stability of the discussed excitation.
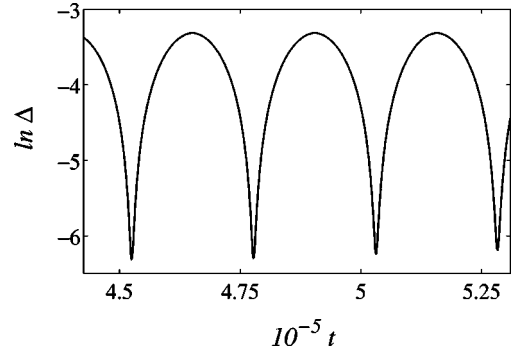

FIG. 10. Time dependence of effective error Δ for the breather solution with $J = 0.1$, $D = -1$, and oscillation period $T = 4.4248$.

For better understanding of the internal breather dynamics, the data are represented through the Fourier expansion of the breather periodic orbit

$$S_n^\alpha(t) = C_0^\alpha(\omega;n) + \sum_{k=1}^{\infty} [A_k^\alpha(\omega;n)\cos k\omega t$$

$$+ B_k^\alpha(\omega;n)\sin \kappa\omega t],$$

$$\alpha = x, y, z. \tag{49}$$

We plot the space configuration of C_0 and $C_n = \sqrt{A_n^2 + B_n^2}$. The ''logarithmic'' profile of such a solution is shown in Fig. 11. We have plotted the space dependence of its Fourier harmonics (from the zeroth to the fifth one) for one particular stable solution.

Let us analyze now the behavior and the exponential spatial decay of these harmonics. As can be seen from Fig. 11, the zeroth (static) component is present. According to this figure, the zeroth component decays exponentially in space. This seems to be surprising because the corresponding zero frequency resonates with the bottom of the acoustic-type linear band [see Eqs. (45) and (46)].

To understand the results illustrated by Fig. 11, we linearize the equations of motion (3) around the ground state (44) in the breather tails. As a result, we obtain the following equations for the S^y and S^z components (S^x is assumed to be equal to 1 with higher-than-linear corrections):

$$-\frac{J}{2|D|}(S_{n+1}^z - 2S_n^z + S_{n-1}^z) + 2S_n^z = 0,$$

$$S_{n+1}^y - 2S_n^y + S_{n-1}^y = 0. \tag{50}$$

The numerical results suggest that the static S_n^y component is zero. This satisfies the second equation in Eq. (50). The first equation in Eq. (50) allows for an exponential decay on the static S_n^z component. Its decay can be characterized by the value λ_0^z if $C_0^z(\omega;n) \sim \exp(-\lambda_0^z|n|), |n| \to \infty, \lambda_0^z > 0$. The substitution of this ansatz into Eq. (45) yields
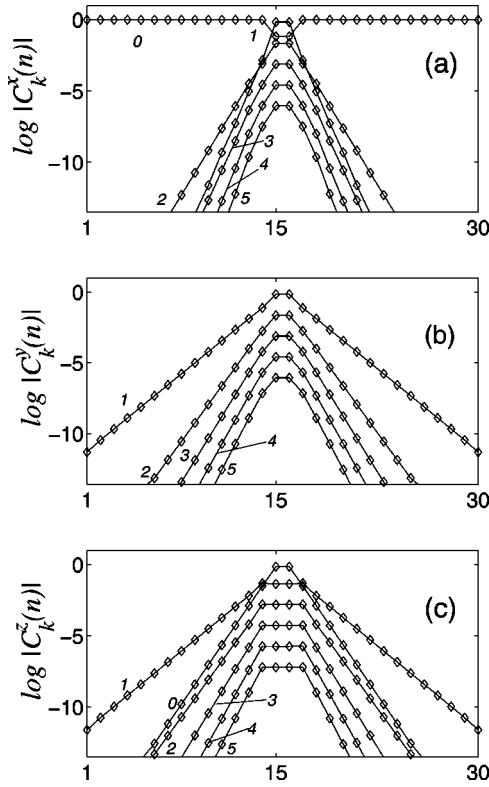
FIG. 11. Spatial dependence of the Fourier components of the discrete breather of the type depicted in Fig. 6 for $J=0.18$, $D=-1$, and $\omega=1.42$. Numbers on the panels represent the order of the harmonic k [see Eq. (49) for explanation].

$$\lambda_0^z=\ln\left[1+\frac{2|D|}{J}+\left\{\left(1+\frac{2|D|}{J}\right)^2-1\right\}^2\right].\qquad(51)$$

The spatial decay of all the other (nonzero) harmonics of the breather solution can be obtained from the dispersion law (45) by substituting $q=\pi-i\lambda^z$ and solving this equation with respect to λ with the frequencies $\Omega_k=k\omega$. As a result, we get

$$\lambda_k^z=\ln[\zeta+\sqrt{\zeta^2-1}]$$

$$\zeta=\frac{\sqrt{D^2+\Omega_k^2}-|D|}{J}-1,\quad k=1,2,\dots.\qquad(52)$$

Since the Fourier components for S_n^y decay in space as S_n^z (except for the static one), we have omitted them. The spatial decay of the Fourier components of S_n^x can be obtained, using the normalization condition (2), and therefore for small deviations from the ground state (44), the following expansion is valid: $S_n^x=1-S_n^{y2}/2-S_n^{z2}/2+O(S_n^{(y,z)4})$. Substituting here the Fourier expansion for S_n^y and S_n^z, one can see that only the product of terms containing harmonics $k\omega$ and ($m\pm k)\omega$ of $S^{y,z}$ will contribute to the decay of the mth harmonic of S^x. We have to choose the smallest exponent of all possible ones, in order to obtain the leading-order decay rate:

TABLE I. Numerically and analytically computed values of the decay exponents λ_k of Fourier harmonics with $k=0,1,\dots,4$ for different spin components. Parameter values are the same as in Fig. 11.

	λ_k^x		$\lambda_k^{y,z}$	
Order, k	Numerical	Analytical	Numerical	Analytical
0	3.5914	3.5903	3.1846	3.1856
1	4.9463	4.8055	1.8067	1.7951
2	3.5859	3.5903	2.9979	3.0103
3	4.8499	4.8055	3.5597	3.5690
4	5.4393	5.3641	3.9195	3.9309

$$\lambda_m^x=\min_{k=0,1,\dots,m}[\lambda_k^z+\lambda_{m\pm k}^z].\qquad(53)$$

As a result, the following relations have been obtained for the first five harmonics of the S^x component: $\lambda_0^x=2\lambda_1^z$, $\lambda_1^x=\lambda_1^z+\lambda_2^z$, $\lambda_2^x=2\lambda_1^z$, $\lambda_3^x=\lambda_1^z+\lambda_2^z$, and $\lambda_4^x=\lambda_1^z+\lambda_3^z$. The comparison of these theoretical results with the values of λ extracted from the numerical data is given in Table I.

As can be seen from Table I, the agreement between the numerical and analytical values of λ decreases with the order of the Fourier components, which can be thought to occur due to the smallness of the higher-order components.

V. TWO-DIMENSIONAL LATTICE WITH EASY-PLANE ANISOTROPY

Finally, we briefly consider a two-dimensional system, namely, an easy-plane ferromagnet with nearest-neighbor exchange interactions. We have numerically simulated the Landau-Lifshitz equations for this system given by

$$\begin{aligned}\dot{S}_{mn}^x=&J_yS_{mn}^z(S_{m-1,n}^y+S_{m+1,n}^y+S_{m,n-1}^y+S_{m,n+1}^y)\\&-J_zS_n^y(S_{m-1,n}^z+S_{m+1,n}^z+S_{m,n-1}^z+S_{m,n+1}^z)\\&-2DS_{mn}^yS_{mn}^z,\end{aligned}$$

$$\begin{aligned}\dot{S}_{mn}^y=&J_zS_{mn}^x(S_{m-1,n}^z+S_{m+1,n}^z+S_{m,n-1}^z+S_{m,n+1}^z)\\&-J_xS_{mn}^z(S_{m-1,n}^x+S_{m+1,n}^x+S_{m,n-1}^x+S_{m,n+1}^x)\\&+2DS_{mn}^xS_{mn}^z,\end{aligned}$$

$$\begin{aligned}\dot{S}_{mn}^z=&J_xS_{mn}^y(S_{m-1,n}^x+S_{m+1,n}^x+S_{m,n-1}^x+S_{m,n+1}^x)\\&-J_yS_{mn}^x(S_{m-1,n}^y+S_{m+1,n}^y+S_{m,n-1}^y+S_{m,n+1}^y),\end{aligned}$$

$$(54)$$

using again the fourth-order Runge-Kutta scheme with various initial-spin configurations. The results of our simulations to some extent are similar to the one-dimensional problem. In Fig. 12, we show the simplest possible configurations of the breathers that involve four out-of-plane precessing spins. No stable breathers with one precessing spin are possible, similarly to the one-dimensional model. Also, there are no
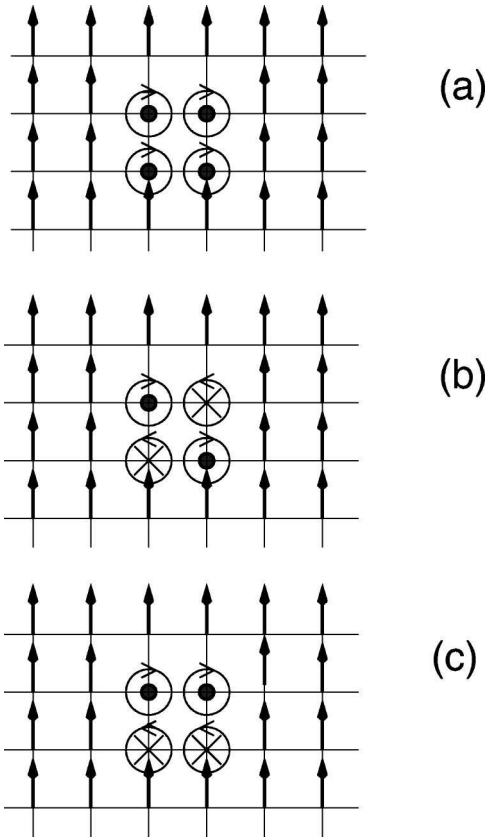
FIG. 12. Schematical representation of some possible configurations of discrete breathers with four processing spins.

stable breathers with two or three precessing spins (at least, in the limit of small J). Among the three possible stable configurations shown in Fig. 12, the first one [see panel (a)] corresponds to four spins precessing parallelly and in-phase, similar to its one-dimensional counterpart. The second two configurations do not have analogs in the one-dimensional case, but they have also similar parity properties. The cases shown in Figs. 12(b) and 12(c) represent the breathers with two spins precessing around the Z axis in the positive direction (marked by dots) and two spins precessing around the negative direction (marked by crosses). The simulations have been performed on a lattice of 150×150 spins with $J = 0.11$ and $D = -1$.

Here we also would like to note that in two-dimensional square-lattice ferromagnets vortices may exist. They are topological solutions of the system and have infinite energy. Since the breathers are excitations whose energy is finite, we do not expect vortices to appear in our simulations. We have excited the 2D breathers by turning corresponding spins out of the easy plane locally and observed only localized excitations accompanied by rapidly decaying radial small-amplitude waves. Note that the properties of the breathers do not depend on the size of the system.

VI. SUMMARY AND DISCUSSIONS

Summarizing, we have considered the breathers in different (easy-axis and easy-plane) classical ferromagnetic spin lattices as essentially discrete objects. We have shown systematically how to implement the anticontinuum limit for different types of magnetic lattices (different types of anisotropy). Depending on the type of anisotropy, the discrete breathers have properties similar to the breather solutions for other nonlinear lattices. In the case of an easy-axis anisotropy, the breather solution appears in the gap of the linear magnon band as do the breathers of the Klein-Gordon-type models. In the easy-plane case, there is no gap in the linear band and the breather frequency lies above the band; these breathers resemble the breathers of the FPU-type chains (also known as the Sievers-Takeno[22] modes).

The concept of the anticontinuum limit helps us, first, to show rigorously the existence of discrete breathers, and, second, to compute the breather solutions numerically. The existence proof has been performed for the one-dimensional *XYZ* Heisenberg ferromagnetic chain with strong exchange ($J_{x,y} \ll J_z$). The proof can easily be generalized to the presence of an easy-axis ion anisotropy and to larger lattice dimensions. The numerical continuation of the solutions from the AC limit has been done with the help of a Newton iteration scheme. Note that so far[12] only the breathers with one nonzero Fourier component in time (43) have been studied, due to the fact that it is much easier to treat them both numerically and analytically. The solutions we have studied allow for the infinite number of harmonics, as in *XYZ* model, for example.

Why is it important to study discrete systems if the continuum approximation can give an analytical solution? First of all, it is known that the breathers are nongeneric for most continuous models.[23] Therefore many systems may be incorrectly referred to as those which do not possess breathers. We demonstrated this circumstance for the easy-axis ferromagnet, where the slightest exchange anisotropy in the hard plane leads to loss of breathers in the continuum model, but not in the case of a spatial lattice. In addition, we have obtained the breather solutions for easy-plane ferromagnets, which have simply no continuum analog. This is due to the fact that the spins in the center of the excitation precess around a tilted axis leading to a local tilt of the magnetization.

Finally, we would like to address some important unanswered questions in this area. The first problem is how to treat quantum spin lattices (e.g., when the total spin is too small to treat the lattices classically) and what is the quantum analog of the spin breather. Another important question is the breather's mobility. So far, there is no rigorous existence proof for moving breathers,[24] however, Lai and Sievers[12] have obtained some numerical results for highly mobile spin breathers. Since their results are concerned only with the breathers with one Fourier component in time, it is still questionable whether the breathers with an infinite number of harmonics can freely propagate along the lattice.

[1] S. Flach and C. R. Willis, Phys. Rep. **295**, 182 (1998).

[2] S. Aubry, Physica D **103**, 201 (1997).

[3] R. S. MacKay and J. A. Sepulchre, Physica D **119**, 148 (1998).

[4] E. Trias, J. J. Mazo, and T. P. Orlando, Phys. Rev. Lett. **84**, 741 (2000); P. Binder, D. Abraimov, A. V. Ustinov, S. Flach, and Y. Zolotaryuk, *ibid.* **84**, 745 (2000).

[5] H. S. Eisenberg, Y. Silberberg, R. Morandotti, A. R. Boyd, and J. S. Aitchison, Phys. Rev. Lett. **81**, 3383 (1998); R. Morandotti, U. Peschel, H. S. Eisenberg, and Y. Silberberg, *ibid.* **83**, 2726 (1999).

[6] I. Swanson, J. A. Brozik, S. P. Love, G. F. Strouse, A. P. Shreve, A. R. Bishop, W.-Z. Wang, and M. I. Salkola, Phys. Rev. Lett. **82**, 3288 (1999).

[7] A. Xie, L. van der Meer, W. Hoff, and R. H. Austin, Phys. Rev. Lett. **84**, 5435 (2000).

[8] For reviews, see A. M. Kosevich, B. A. Ivanov, and A. S. Kovalev, Phys. Rep. **194**, 117 (1990), and references therein.

[9] V. G. Makhankov and V. K. Fedyanin, Phys. Rep. **104**, 1 (1984).

[10] S. Takeno and K. Kawasaki, J. Phys. Soc. Jpn. **60**, 1881 (1991); Phys. Rev. B **45**, 5083 (1992).

[11] R. F. Wallis, D. L. Mills, and A. D. Boardman, Phys. Rev. B **52**, R3828 (1995).

[12] R. Lai and A. J. Sievers, Phys. Rep. **314**, 147 (1999).

[13] U. T. Schwarz, L. Q. English, and A. J. Sievers, Phys. Rev. Lett. **83**, 223 (1999).

[14] S. Flach, Physica D **91**, 233 (1996).

[15] R. S. MacKay and S. Aubry, Nonlinearity **7**, 1623 (1994).

[16] Consider a decoupled spin $\mathbf{S}=(S^x,S^y,S^z)$. In the action-angle variables (I,θ), the frequency of the periodic orbit around the stable ground state equals $\omega=dE/dI$, where E is energy of the spin and the dynamics of the associated angle are given by $d\theta/dt=\omega(I)$. The periodic orbit with the action I_0 is *anharmonic* if $d\omega/dI(I_0)\neq 0$.

[17] J. L. Marín, S. Aubry, and L. M. Floría, Physica D **113**, 283 (1998).

[18] B. A. Ivanov, A. M. Kosevich, and I. M. Babich, Pis'ma Zh. Eksp. Teor. Fiz. **29**, 777 (1979) [JETP Lett. **29**, 714 (1979)].

[19] I. M. Babich and A. M. Kosevich, Pis'ma Zh. Eksp. Teor. Fiz. **31**, 224 (1980) [JETP Lett. **31**, 205 (1980)].

[20] S. Flach, K. Kladko, and R. S. MacKay, Phys. Rev. Lett. **78**, 1207 (1997).

[21] K. W. Sandusky, J. B. Page, and K. E. Schmidt, Phys. Rev. B **46**, 6161 (1992).

[22] A. J. Sievers and S. Takeno, Phys. Rev. Lett. **61**, 970 (1988).

[23] H. Segur and M. D. Kruskal, Phys. Rev. Lett. **58**, 747 (1987).

[24] S. Flach and K. Kladko, Physica D **127**, 61 (1999).